

Modeling and Simulation of NO_x Abatement with Storage/Reduction Catalysts for Lean Burn and Diesel Engines

Jan Koop, Olaf Deutschmann

Institute for Chemical Technology and Polymer Chemistry, University of Karlsruhe, Germany

Copyright © 2006 SAE International

ABSTRACT

The removal of nitrogen oxides emitted by diesel and lean burn engines is one of the most important targets in catalytic exhaust aftertreatment research. Besides the selective catalytic reduction (SCR) reaction with ammonia the most promising approach is the NO_x Storage and Reduction Catalyst (NSR) which utilizes the nitrogen oxides storage on barium sites to form nitrates during the lean phase and their reduction to nitrogen in a rich atmosphere.

In this paper, we present a modeling approach for the description of the transient behavior of a NSR. The model applies a two-dimensional description of the flow field in the single channels coupled with detailed models for the chemical processes.

The mechanism used for modeling the oxidation and reduction of carbon monoxide, hydrocarbons, and nitrogen oxides, respectively, is based on an elementary step reaction mechanism for platinum catalysts and a shrinking core model for the storage and reduction processes on the barium particles.

INTRODUCTION

In spite of the enormous achievements in the aftertreatment of exhaust gas emissions, the worldwide increasing number of vehicles represents a serious environmental problem due to vehicles' raw emissions, in particular, carbon dioxide, which has a strong impact on the greenhouse effect. A more efficient fuel consumption can be realized in Diesel and lean-operated engines, i.e., in excess of air (oxygen). Here, the problem is the formation of nitrogen oxides (NO_x). Since improvements of the combustion process itself are not sufficient to meet future legislative limits, the development of a technique for the aftertreatment of NO_x is urgently needed.

One of the most promising approaches is the NO_x Storage and Reduction Catalyst (NSR) which utilizes the NO_x storage on barium sites to form nitrates during the

lean phase and their reduction to nitrogen in a rich atmosphere. Detailed models, which are based on physical and chemical processes on the molecular level, are indispensable to exploit the full potential of this technique.

For the simulation, we apply the DETCHEM software [21] which is a FORTRAN based package that is designed to couple detailed chemistry models and computational fluid dynamics (CFD). The core is a library for the description of species properties based on atomistic models and for reactions among gas-phase and surface species based on elementary step reaction mechanisms. Upon this, the two-dimensional flow field in a single channel is modeled using the boundary-layer assumption. Radial transport models include composition and temperature dependent transport coefficients in the gas phase and an effectiveness factor approach for the washcoat. Inlet conditions and NO_x storage capacities of the single channel simulations vary in time.

The present study aims at detailed insight into the processes on the catalyst surface and their interaction with the transport in the fluid flow at transient conditions by coupling the extensive description of the flow-field with elementary-step mechanisms on the noble metal catalyst and the storage/reduction chemistry on barium. A realistic exhaust gas composition including water and carbon dioxide and using propylene as representative hydrocarbon is exposed to a commercially manufactured model catalysts in order to obtain practical experimental results as a basis for the modeling.

Many studies in recent years have been published on modeling NO_x storage catalysts under varying conditions and with different levels of detail [3,4,5,6,12, and 14]. A short overview is given by Koltsakis [4]. The approaches in literature differ especially in the applied reaction mechanisms, e.g. either global reaction or elementary-step like. Also, the flow field is often simulated by a one-dimensional description neglecting transport limitation of the overall reaction rate. Furthermore, most studies consider only NO oxidation in the lean phase and its

reduction in the rich phase. The applied gas matrix is often far away from a realistic exhaust gas, because it contains neither water nor CO₂, both have a strong influence on the catalytic activity of the noble metal and the morphology of barium [2,15].

One approach for the simulation of NO_x storage is the idea of shrinking core model. Since the storage of nitrogen oxides is a slow process compared with the subsequent reduction, the observed behavior can be explained with the different molar volumes of BaCO₃ and Ba(NO₃)₂ [1]. Hepburn et al. [5] suggested a kinetic model to account for slow diffusion of reactants into the barium particles. We have implemented a shrinking core model for the description of internal mass transport effects based on the kinetic rate expressions derived by Olsson et al [3].

MATHEMATICAL AND NUMERICAL MODEL

The numerical model for the simulation of the NSR catalyst consists of two parts. Since the time scale of the catalytic reactions on the noble metal is much smaller than the slow storage reactions, these two processes can be decoupled. Thus, the catalytic surface reactions are considered to be in quasi-steady state at given local species concentrations and temperature, while for the surface species involved in the storage process transient species equations are solved. The chemistry module DETCHEM^{RESERVOIR} [21] has been applied for modeling of the flow field and the reactions on the surface.

FLOW FIELD MODEL

The reactive flow field in the single catalytic channel with cylindrical symmetry is modeled by the steady state, two-dimensional boundary layer equations [7,21]. Surface reactions are modeled by an elementary-step reaction mechanism based on the molecular processes using the mean-field approximation.

In the boundary layer of a fluid near a surface, the convection is mainly directed parallel to the surface. The diffusive transport in the same direction diminishes in comparison with the one perpendicular to the surface. This effect becomes more significant as the axial gas velocity is increased, i.e. for higher Reynolds numbers as long as the flow is laminar. The results achieved by the boundary-layer model can be as accurate as the results from the full Navier-Stokes model at high but laminar flow rates [10].

Usually the surface of the solid catalyst is coated with a layer of high surface area material, the washcoat, in which the catalyst is dispersed. The washcoat thickness varies from 10 to 150 μm and can exhibit a non-uniform thickness around the perimeter of the cell. Transport of chemical species inside the washcoat is taken into account by applying an effectiveness factor, η , which depends on the porosity, gas-phase species concentrations at the fluid/washcoat boundary, surface

reaction rates, and diffusion coefficients using the Thiele module approach [20].

Our model approach leads to the following conservation equation for a single channel simulation

Continuity equation

$$\frac{\partial(\rho u)}{\partial z} + \frac{1}{r} \frac{\partial(r \rho v)}{\partial r} = 0 \quad (1)$$

Axial momentum

$$\rho u \frac{\partial(u)}{\partial z} + \rho v \frac{\partial(u)}{\partial r} = -\frac{\partial p}{\partial z} + \frac{1}{r} \frac{\partial}{\partial r} \left(\mu r \frac{\partial u}{\partial r} \right) \quad (2)$$

Species conservation equation

$$\rho u \frac{\partial(Y_i)}{\partial z} + \rho v \frac{\partial(Y_i)}{\partial r} = \frac{1}{r} \frac{\partial(r j_{i,r})}{\partial r} \quad (3)$$

with the diffusion mass flux at the interface of free fluid flow and washcoat being

$$j_{i,r} = \eta \cdot \dot{s}_i \cdot \tilde{M}_i \cdot F_{cat/geo} \quad (4)$$

$F_{cat/geo}$ denotes the ratio between the catalytic surface area of the noble metal or storage component and the geometrical area of the catalyst. The transport coefficients (μ , λ) and the radial species diffusion fluxes $j_{i,r}$ depend on temperature and gas-phase composition.

The transient behavior of the NSR is modeled by an external time – loop having the inlet conditions, and the locally resolved storage species as transient variables. At each time step, the 2d flow field and the reaction rates on the noble metal catalyst are calculated. The external loop then updates the transient coverages Θ_i of the storage component:

$$\frac{\partial \Theta_i}{\partial t} = \frac{\dot{s}_i}{\Gamma} \quad (5)$$

with a general surface reaction rate

$$\dot{s}_i = \sum_{k=1}^{K_s} \nu_{ik} k_{fk} \prod_{j=1}^{N_g+N_s} c_j^{\nu'_{jk}} \quad (6)$$

SURFACE CHEMISTRY MODEL

The chemical source terms due to surface reactions ($j_{i,r}$, \dot{S}_i) in Eqs. 3 and 4 are modeled by elementary-step based reaction mechanisms. The applied chemistry model for the reactions on platinum is only discussed briefly; a more comprehensive description and examples for its application can be found elsewhere [7, 8, 9, and 11].

The state of the catalytic surface is described by its temperature and the coverage of adsorbed species which vary along the channel. The chemical source terms \dot{S}_i of gas phase species due to adsorption/desorption and surface species are given by Equation 5 and 6. The surface reactions on the noble metal are assumed to be in steady-state, thus, Equation 5 is set equal to zero in this case.

The temperature dependence of the rate coefficients is described by a modified Arrhenius expression:

$$k_{fk} = A_k T^{\beta_k} \exp\left[\frac{-E_{ak}}{RT}\right] \prod_{i=1}^{N_s} \Theta_i^{\mu_{ik}} \exp\left[\frac{\varepsilon_{ik} \Theta_i}{RT}\right] \quad (7)$$

This expression takes the coverage dependence of the rate constants, e.g. activation energy, into account using the parameters μ_{ik} and ε_{ik} .

The rate of reaction for an adsorption processes is calculated from the sticking coefficient S_i^0 :

$$k_{fk}^{ads} = S_i^0 \frac{1}{\Gamma} \sqrt{\frac{RT}{2\pi\tilde{M}_i}} \quad (8)$$

The elementary step reaction scheme which is applied for the simulation of the oxidation and reduction reactions on platinum is based upon a previously published mechanism [11]. Since in this study an extended gas matrix was used for the simulated exhaust gas, reactions of nitrogen oxides with hydrogen and steam reforming reactions were added. The developed surface reaction mechanism consists of 70 elementary reaction steps among 35 surface and 10 gas phase species. Furthermore, the kinetic data of the detailed reaction mechanism have been modified in order to accomplish a thermodynamic consistent data set. The values for the pre-exponential factors and activation energies of the elementary step mechanism published by Chatterjee et al [11] were taken mostly from literature (e.g. surface science experiments and quantum chemical calculations). However, for some reactions the kinetic data had to be estimated and then refined according to the experimental results, because no reliable kinetic data were available in literature.

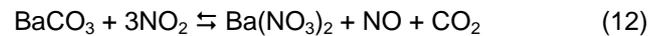
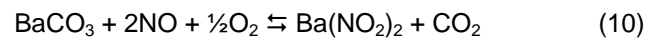
The applied elementary-step mechanism includes dissociative adsorption of O_2 and non-dissociative adsorption of NO , NO_2 , N_2O , CO , H_2 , CO_2 , C_3H_6 , H_2O and desorption of all species. Gas-phase reactions do not take place due to the low pressure and temperature in automotive catalytic converters. All reactions on platinum are modeled as reversible reactions and the developed mechanism consists of four parts. The decomposition of propylene via abstraction of hydrogen atoms, the oxidation of carbon monoxide to carbon dioxide and the formation of water via an adsorbed hydroxyl species (OH), respectively, reaction between oxygen and hydrogen. Formation of nitrogen dioxide occurs by oxidation of nitric oxide and depletion by reduction with hydrogen to NO and further to N_2 . The oxidation of nitric oxide is modeled by both a Langmuir-Hinshelwood and an Eley-Rideal mechanism.

NO_x STORAGE MODEL

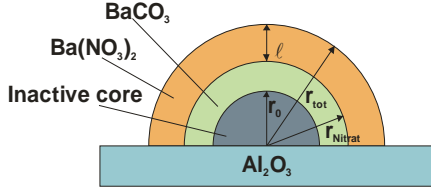
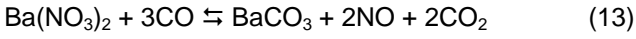
The uptake of NO_x on barium sites is modeled by a shrinking core model [3] with an inactive core. The storage of nitrogen oxides is characterized by an initial complete uptake and a slow increase of the NO_x concentration at the end of the catalyst due to the depletion of available storage sites. However, the reduction of the stored nitrogen oxides is a very fast process. The difference in timescales is a result of the slow diffusion of NO_x through the porous structure into the barium particle. Due to the difference of molar volumes of $BaCO_3$ and $Ba(NO_3)_2$, the particles are assumed to become denser during their transformation from carbonates to nitrates [1]. Furthermore, after a certain time the pore volume decreases and the inner part of the large barium particle is no longer accessible for the gas. During regeneration the particles break up and form clefts which enable fast diffusion of the reactants.

For the simulation the storage process is described by the reaction of mainly nitrogen dioxide with barium carbonate to form nitrates. However, also a direct reaction of nitric oxide and oxygen to nitrites is included in order to account for the experimental observation of $Ba(NO_2)_2$ [17,18]. The barium nitrite is only an intermediate, because nitrates are dominant after long exposure.

Storage Reactions:



Reduction Reactions:



A detailed description and derivation of the kinetic expressions are given by Olsson [3]. Exemplary for reaction (9) the following rate expression can be derived:

$$\dot{r}_{\text{NO}_2-\text{O}_2-\text{Ba}} = \tilde{k}_f * c_{\text{NO}_2} * c_{\text{O}_2}^{0.25} * \Theta_{\text{BaCO}_3} - \tilde{k}_b * c_{\text{CO}_2}^{0.5} * \Theta_{\text{Ba}(\text{NO}_3)_2} \quad (16)$$

$$\tilde{k}_f = \frac{k_f}{1 + k_f * \tau} \quad \tilde{k}_b = \frac{k_b}{1 + k_b * \tau} \quad (17)$$

$$k_f = A_f * T^\beta * e^{-\frac{E_{a,f}}{RT}} \quad (18)$$

$$k_b = \frac{k_f}{K_{\text{NO}_2-\text{O}_2-\text{Ba}}^{\text{eq}}} = \frac{k_f}{\exp\left(-\frac{\Delta_R H}{RT} + \frac{\Delta_R S}{R}\right)} \quad (19)$$

$$\tau = \frac{\ell}{D} * \frac{r_{\text{Nitrate}}}{r_{\text{tot}}} \quad (20)$$

The rate coefficient of the forward reaction is modeled by a simple Arrhenius expression with a pre-exponential factor and activation energy. The reverse reaction is expressed in terms of the equilibrium constant for the reaction which in turn is a function of the reaction enthalpy and entropy. As more nitrates are formed during the storage process the reaction front migrates deeper into the particle and the thickness of the barium nitrate layer ℓ increases. Thus, the term τ ascends which gives rise to a decreased rate expression. The diffusion coefficient D which describes the transport of nitrogen oxides within the barium particles varies strongly with temperature and has been fitted to the experiments. The data for the reaction enthalpy and entropy have been taken from a thermodynamic data basis [16].

The three storage reactions (9, 10, and 12) are modeled with the shrinking core based rate expressions derived in Equations 17 to 20. However, the conversion of barium nitrite to nitrate is a fast process and thus modeled as a global reaction with a simple Arrhenius type rate coefficient. Furthermore, it is significant for the shrinking core model that the reduction reactions in the rich phase are much faster than the storage reactions in the lean phase. The regeneration of the barium nitrate like the oxidation of nitrite to nitrate is therefore modeled by global reactions with Arrhenius expression but without any inhibition term.

EXPERIMENTAL

The experimental work, which was accomplished at the Institute for Chemical Process Engineering at the University of Stuttgart [22], is based on well-defined model catalysts of monolithic structure and of varying complexity. The catalysts are manufactured with commercial techniques and were provided by Delphi Catalyst. The samples have been hydrothermally aged for 4h at 700°C. The specifications of the substrate, the coating and the dimensions are listed below.

Table 1: Catalyst Specifications

Substrate	
Material	Cordierite
Length	0.2 m
Width	0.03 m
Height	One channel
Cell density	62 cm ⁻² (400 cpsi)
Coating	
Washcoat	γ -Alumina
Noble Metal	Platinum (80 g/ft ³)
Storage Component	Barium
BET Surface Area of Pt/Al ₂ O ₃	49.4 m ² /g
BET Surface Area of Pt/Ba/Al ₂ O ₃	45.8 m ² /g

These model catalysts have been extensively characterized by BET, mercury porosimetry, CO-Chemisorption, TEM, EDX, and XRD. The BET surface decreases upon addition of barium to the platinum

containing sample, which was also reported in literature [23]. The dispersion of platinum determined by CO-chemisorption is 16% for the Pt/Al₂O₃ sample. The XRD experiments showed that barium is found in the form of carbonate only. Furthermore, TEM measurements revealed the size of the barium particles to be approximately 100 nm.

The investigations of the kinetics are carried out under isothermal conditions in a flat bed reactor [22] using a realistic model exhaust gas, given in Table 2. Furthermore, lateral outlets allow the measurement of gas concentration profiles along the length of the catalyst. The experimental system is equipped with a fast responding mass spectrometer for the measurement of short lean/rich cycles. The space velocity is 40000 h⁻¹.

Table 2: Composition of the gas matrix

Gas	Lean	Rich
NO [ppm]	200	200
NO ₂ [ppm]	40	40
O ₂ [Vol.-%]	12	0.9
C ₃ H ₆ [ppm]	60	60
CO [Vol.-%]	0.04	2.1
CO ₂ [Vol.-%]	7	7
H ₂ O [Vol.-%]	10	10
H ₂ [Vol.-%]	0	0.7

Experiments have been conducted for Pt/Al₂O₃ and Pt/Ba/Al₂O₃ samples in the temperature range of 150 to 450 °C for varying duration of lean/rich cycle (60s/5s and 300s/15s). Additionally, long-term storage experiments with barium containing catalysts were performed.

RESULTS AND DISCUSSION

PLATINUM ON ALUMINA

In the simulation, the conditions summarized in Table 3 are used as input data. The gas flows with a uniform inlet velocity into the cylindrical tube. Due to the constant sample temperature in the experiments, the channel wall is assumed to be isothermal. In order to account for the diffusion of the reactants into the washcoat an effectiveness factor model has been applied with NO as the diffusion determining molecule. The results of the simple model have been compared to a detailed washcoat model with species profiles and surface coverages spatially resolved inside the washcoat layer. The simulations (results are not shown here) revealed

only slight differences between the effectiveness factor and the detailed model concerning the outlet concentrations. Therefore the computationally less expensive effectiveness factor model was applied for most of the simulations.

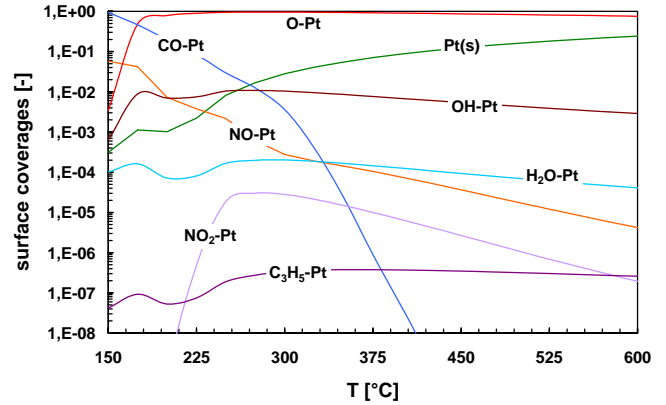


Figure 1: Surface coverages on platinum as a function of temperature; lean phase

Table 3: Input data for the simulations

Noble Metal loading	80 g/ft ³
Noble Metal dispersion	16 %
Ratio active surface area/ geometrical surface ($F_{cat/geo}$)	41
Surface site density (Pt)	2.72×10^{-9} mol/cm ²
Channel diameter	1.0 mm
Channel length	0.2 m
Velocity (temperature- dependent)	3.38 m/s at 25°C

Simulations of the Pt/Al₂O₃ catalyst were performed at temperatures of 250, 350, and 450°C for lean/rich cycle of 300s/15s with the gas-phase concentrations given in Table 2. The program DETCHEM^{RESERVOIR} [21] is used for the simulation of the lean/rich cycles. In addition to the isothermal simulations, a temperature ramp study with the same input data has been accomplished in order to obtain information about the surface coverage at the corresponding temperature. The computed temperature ramp runs from 150 to 600°C. The results are shown in Fig. 1. At low temperature the platinum surface is mainly covered with CO and to a lower extent with atomic oxygen. As the oxidation of carbon

monoxide proceeds, oxygen becomes the predominant adsorbed species on the surface. After the light-off of the CO oxidation the conversion of NO to NO₂ takes place indicated by the depletion of the NO-Pt species. Thus, at about the 270°C the number of free platinum sites Pt(s) increases significantly.

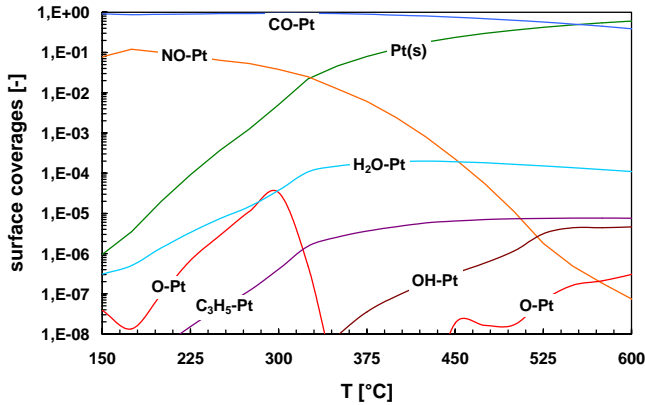


Figure 2: Surface coverages on platinum as a function of temperature; rich phase

The calculated surface coverages on platinum in the rich phase are displayed in Figure 2. The surface is mainly covered with carbon monoxide over the whole temperature range due to the high sticking coefficient on platinum [11]. At 300°C the reduction of nitric oxide starts leading to an increasing number of free platinum sites whereas the reduction of nitrogen dioxide by hydrogen is already completed for temperatures below 250°C.

The modeling results of the lean/rich cycles are shown for a selected temperature of 350°C in Figure 3. The simulated data are compared to the results of the experimental investigation. The predicted concentrations agree well with the experimentally measured data. Displayed are the outlet concentrations at isothermal conditions of nitrogen oxides, propylene, and oxygen as a function of cycle time. Since the experimental data show only little variation with time, it is justified to assume the surface reaction to be in steady-state. In the lean phase, all hydrocarbons are oxidized and the NO is mainly converted to NO₂ at this temperature of 350°C. The beginning of the rich phase is denoted by the sharp drop of the O₂ concentration. In the oxygen deficit atmosphere, the nitrogen oxides are reduced to nitrogen by hydrogen as well as by carbon monoxide. Side reactions to ammonia or nitrous oxide are not included. The CO competes with the propylene for the oxygen, but since the surface at this temperature is mainly covered with carbon monoxide, not enough free platinum sites are available for the adsorption of the C₃H₆ species and its further oxidation.

At 350°C the mole fraction of NO, NO₂, and C₃H₆ for the lean mixture within the channel are depicted in Figure 3. For all three species the radial gradients are negligible. The conversion of NO to NO₂ increases linearly along the axial direction and is completed at half of the catalyst length. The oxidation of the propylene is much faster which is revealed by the complete conversion in the first three centimeters of the catalyst channel.

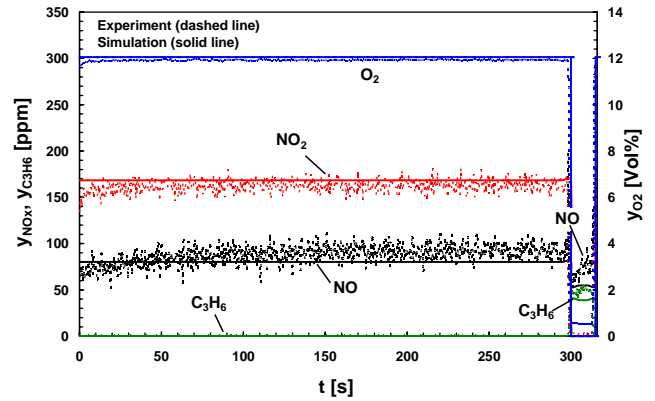


Figure 3: Lean/rich cycle (300s/15s) of Pt/Al₂O₃ catalyst at 350°C; comparison of experimental and simulated data

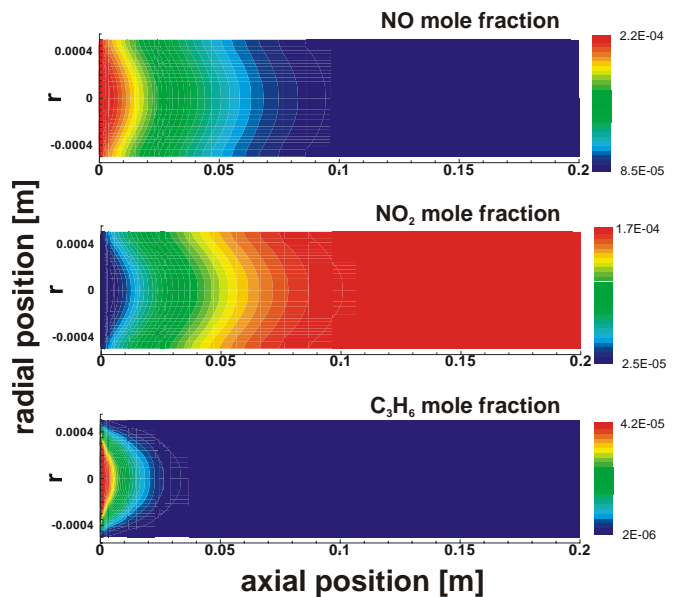


Figure 4: Flow fields of the mole fraction of the species NO, NO₂ and C₃H₆ at 350°C. Different scales are used in axial and radial direction for visual clarity; lean mixture

PLATINUM AND BARIUM ON ALUMINA

For the simulation of the entire NO_x storage catalyst the elementary-step mechanism for the platinum only catalyst was extended by the global reactions for the NO_x storage and reduction on barium, Equations 9 to 15. Numerical simulations were carried out under isothermal conditions at 250, 350, and 450°C.

In this study, numerical simulation results for a Pt/Ba/Al₂O₃ catalyst are presented. The feed stream is cycled between lean (60s) and rich (5s) conditions, which is a realistic time scale in automotive application. Input data and gas composition are the same as in the previous section and are given in Tables 2 and 3, respectively. However, the ratio of active metal surface to geometrical surface for platinum, $F_{cat/geo}$, is adjusted in order to account for the lower catalytic activity of the Pt/Ba/Al₂O₃ sample. The factor $F_{cat/geo}$ in Equation 4 influences directly the surface reaction rate and was estimated to be 10 for the barium containing catalyst. Our findings are in accordance with literature results, which show that the addition of barium leads to a significantly reduced NO and hydrocarbon oxidation activity. The negative effect can not only be ascribed to the reduced surface area upon addition of barium. Olsson and Fridell suggested that the alkalinity of the barium support leads to exaggerated formation of platinum oxide in comparison to Pt/Al₂O₃[19].

The kinetic data A_i and $E_{a,i}$ for the storage and reduction reactions and the diffusion coefficient, D , within the barium particles have been obtained from comparison with the experimental data of the lean/rich cycles as well as long-term storage experiments (not depicted). In these measurements a fully regenerated catalyst sample has been treated with the gas matrix given in Table 3 for 5000 seconds. The rate constants of the reverse storage reactions are calculated from thermodynamic data, i.e. reaction enthalpies and reaction entropies, which have been taken from literature [16]. For barium nitrite no literature data for the entropy is available, therefore the value is adjusted to the experiments.

In Figures 5 to 10 a comparison between experimental and modeling results at 250, 350, and 450°C are shown. The experimental results are obtained after the catalyst has reached steady-state, i.e. the sample has been cycled until no change in outlet concentration between the cycles was detected anymore.

For all displayed temperatures the simulated concentrations match the experimental data well. In the lean period, the NO_x inlet concentration is 240 ppm. At 250°C the overall storage efficiency is about 30% and almost constant during the lean phase. Whereas at 350 and 450°C, even at the end of the 60 second lean phase almost 80% of the inlet nitrogen oxides are stored. At these temperatures the profile of the NO_x concentration is characterized by an almost complete uptake in the first 20 seconds. After this, the NO_x which break through ascends because the pores of the barium cluster close

due to the volume increase and the depletion of the carbonate. In the rich phase all the stored nitrogen oxides are released into the gas phase.

At 250°C the subsequent reduction of the nitric oxides with carbon monoxide or hydrogen is kinetically limited, thus, a big NO peak is observable. At higher temperatures the reaction rate of the reduction increases and after a smaller NO peak no nitrogen oxides break through. In addition, at higher temperature the nitrates become thermodynamically unstable, hence, the height of the NO peak is greater at 450°C than at 350°C.

In Figures 8 to 10, a comparison of simulation and experimental results of the axial profiles for NO, NO₂, and C₃H₆ at 350°C are depicted. The NO concentration decreases monotonically along the catalyst length due to the oxidation to nitrogen dioxide. However, the profile of NO₂ exhibits a different behavior. In the first half of the channel the concentration rises but in the second half the influence of the storage reactions preponderates. Furthermore, there is also a variation in the concentration profile with time for both NO and NO₂. The conversion of propylene is very fast compared with the oxidation of NO and is completed within the first centimeters of the channel length.

The distributions of barium nitrate along the catalyst length as a function of time are depicted in Figures 10 to 12 for three different temperatures. The Figures show the simulated coverages of the second lean/rich cycle (60s/5s). The input coverages for the depicted cycle are obtained from the previous lean/rich run. At all three temperatures the Ba(NO₃)₂ coverages increase with time due to the storage reactions. The distribution along the channel length, however, is not uniform because at the catalyst entrance more nitrates are stored than at the end. At 350 and 450°C almost all carbonates are converted to nitrates within the first five centimeters. In contrast, the nitrate coverage in the last five centimeters does not exceed 20 percent at all three investigated temperatures. Switching after 60 seconds lean gas mixture to a short rich gas matrix is indicated by the sharp decrease in the nitrate coverage due to the reduction reactions. At lower temperatures the reduction of the barium nitrates are slow, which give rise to a high Ba(NO₃)₂ residual, especially at the catalyst entrance.

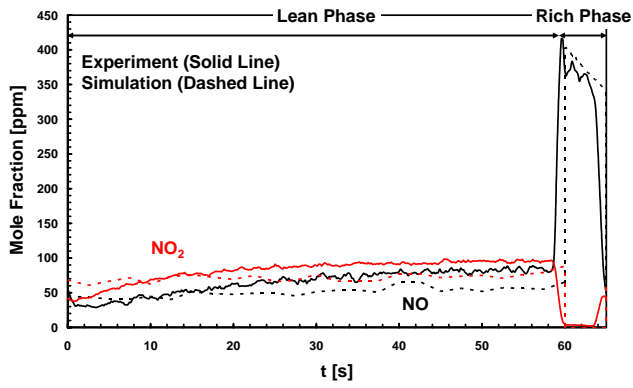


Figure 5: Lean/rich cycle (60s/5s) of Pt/Ba/Al₂O₃ catalyst at 250°C; comparison of experimental and simulated data

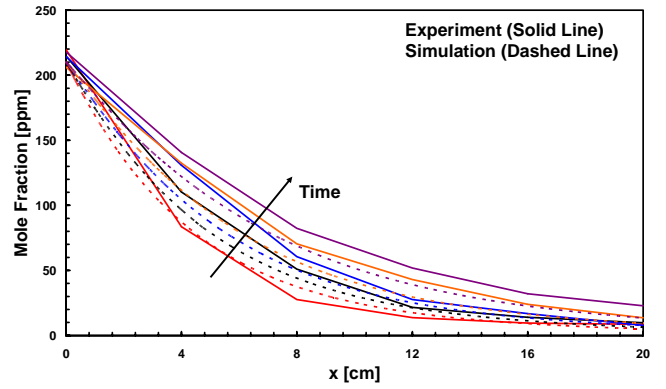


Figure 8: Axial profile of the NO concentration at a particular time in the lean phase of Pt/Ba/Al₂O₃ catalyst at 350°C

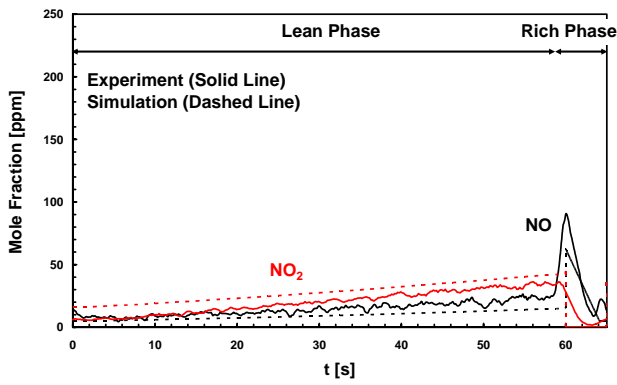


Figure 6: Lean/rich cycle (60s/5s) of Pt/Ba/Al₂O₃ catalyst at 350°C; comparison of experimental and simulated data

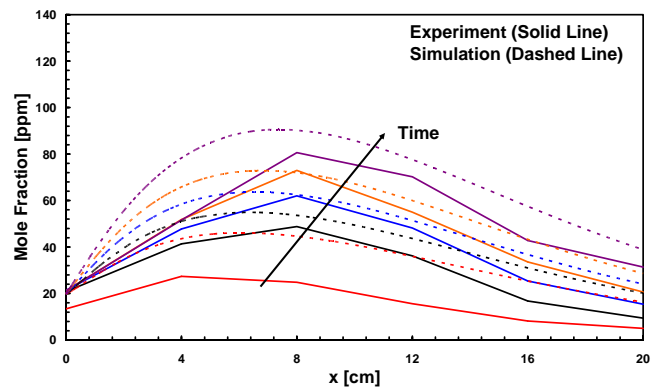


Figure 9: Axial profile of the NO₂ concentration at a particular time in the lean phase of Pt/Ba/Al₂O₃ catalyst at 350°C

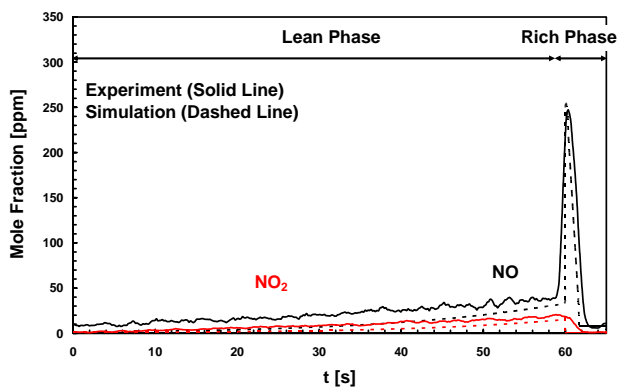


Figure 7: Lean/rich cycle (60s/5s) of Pt/Ba/Al₂O₃ catalyst at 450°C; comparison of experimental and simulated data

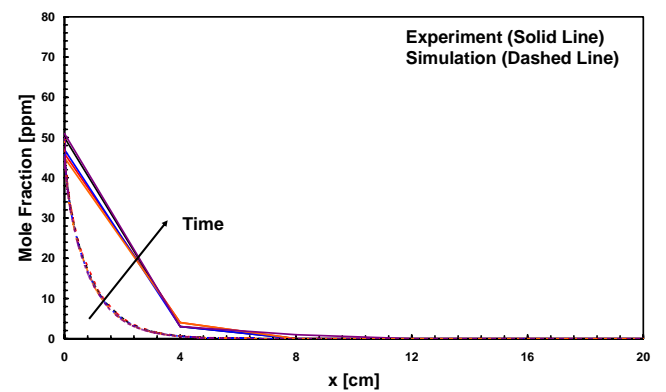


Figure 10: Axial profile of the C₃H₆ concentration at a particular time in the lean phase of Pt/Ba/Al₂O₃ catalyst at 350°C

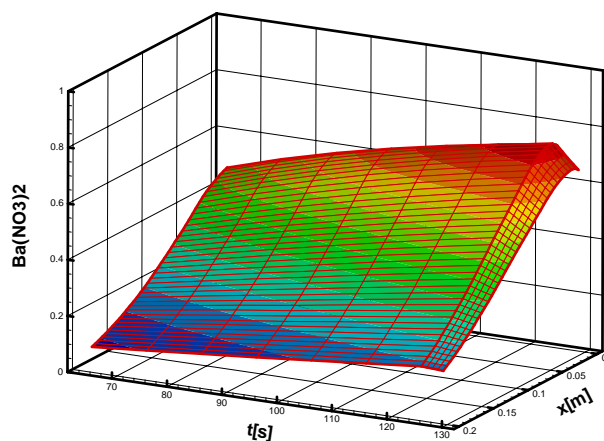


Figure 11: Axial and temporal profile of the simulated coverage with $\text{Ba}(\text{NO}_3)_2$ for a Pt/Ba/ Al_2O_3 catalyst at 250°C

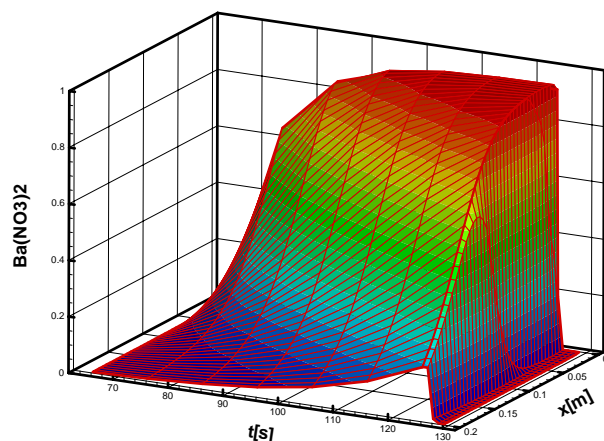


Figure 13: Axial and temporal profile of the simulated coverage with $\text{Ba}(\text{NO}_3)_2$ for a Pt/Ba/ Al_2O_3 catalyst at 450°C

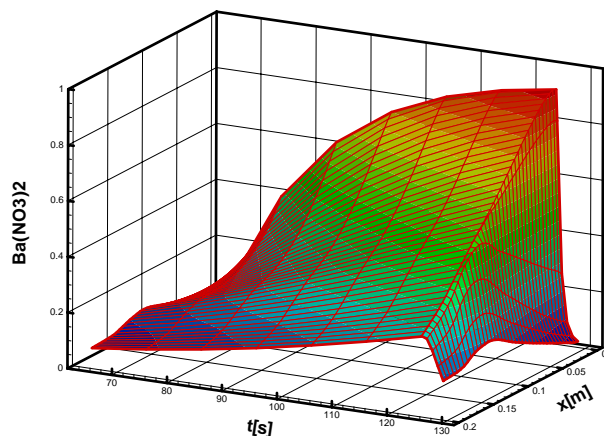


Figure 12: Axial and temporal profile of the simulated coverage with $\text{Ba}(\text{NO}_3)_2$ for a Pt/Ba/ Al_2O_3 catalyst at 350°C

CONCLUSION

The recently developed computational tool DETCHEM^{RESERVOIR} is applied for the transient simulation of lean/rich cycles of a NO_x storage and reduction catalyst. The numerical code is based on a two dimensional description (boundary-layer approximation) of the flow field in the single channel of a monolith coupled with a detailed reaction mechanism for the conversion of CO, C_3H_6 , and NO_x on platinum and a shrinking core model for the storage of nitrogen oxides on barium. Included is also a washcoat model.

The computational tool was used to simulate the oxidation and reduction reactions of a platinum-only catalyst at various temperatures. The model enables the prediction of the concentration profiles along the channel length and gives a detailed insight into the surface coverages of the lean and rich phase, respectively.

Based upon the reactions on the noble metal and a shrinking core model for the NO_x storage, transient numerical simulations have been accomplished in order to predict the performance of the NSR in a temperature range from 250 to 450°C. The model predicts the experimentally measured concentration profiles in the lean as well as in the rich phase quite well. Simulated distribution of barium nitrate along the catalyst length as a function of time revealed that the storage in the first half of the channel is more pronounced than in the second half. Furthermore, at lower temperatures the regeneration of the catalyst is incomplete due to slow reduction reactions which result in a $\text{Ba}(\text{NO}_3)_2$ residual.

OUTLOOK

We are currently working on the extension of the numerical simulation model of the NO_x storage catalyst by a model for the oxygen storage on ceria.

ACKNOWLEDGMENTS

The authors would like to gratefully acknowledge the Forschungsvereinigung Verbrennungskraftmaschinen e.V. (FVV) for the financial support and Delphi Catalyst for providing the model catalysts. The authors would also like to thank Volker Schmeißer and Gerhart Eigenberger (University of Stuttgart) for sharing their experimental results which are crucial for the success of this work.

REFERENCES

1. U. Tuttlies, V. Schmeisser and G. Eigenberger, "A mechanistic simulation model for NO_x storage catalyst dynamics," *Chemical Engineering Science*, Vol. 59, No. 22-23 (2004), pp. 4731-4738.
2. N. W. Cant and M. J. Patterson, "The Effect of Water and Reductants on the Release of Nitrogen Oxides Stored on BaO/Al₂O₃," *Catalysis Letters*, Vol. 85, No. 3-4 (2003), pp. 153-157.
3. L. Olsson, R. J. Blint and E. Fridell, "Global Kinetic Model for Lean NO_x Traps," *Industrial & Engineering Chemistry Research*, Vol. 44, No. 9 (2005), pp. 3021-3032.
4. G. C. Koltsakis, N. Margaritis, O. Haralampous and Z. C. Samaras, "Development and Experimental Validation of a NO_x Trap Model for Diesel Exhaust," *SAE Paper 2006-01-0471*.
5. J. S. Hepburn, E. Thanasiu, D. A. Dobson and W. L. Watkins, "Experimental and Modeling Investigations of NO_x Trap Performance," *SAE Paper 962051*.
6. P. Koci, M. Marek, M. Kubicek, T. Maunula and M. Harkonen, "Modelling of catalytic monolith converters with low- and high-temperature NO_x storage compounds and differentiated washcoat," *Chemical Engineering Journal*, Vol. 97, No. 2-3 (2004), pp. 131-139.
7. J. Braun, T. Hauber, H. Többen, J. Windmann, P. Zacke, D. Chatterjee, C. Correa, O. Deutschmann and J. Warnatz, "Three-Dimensional Simulation of the Transient Behavior of a Three-Way Catalytic Converter," *SAE Paper 2002-01-0065*.
8. J. Braun, T. Hauber, H. Többen, P. Zacke, D. Chatterjee, O. Deutschmann and J. Warnatz, "Influence of Physical and Chemical Parameters on the Conversion Rate of a Catalytic Converter: a Numerical Simulation Study," *SAE Paper 2000-01-0211*.
9. J. Windmann, J. Braun, P. Zacke, S. Tischer, O. Deutschmann and J. Warnatz, "Impact of the inlet flow distribution on the light-off behavior of a 3-way catalytic converter," *SAE Paper 2003-01-0937*.
10. L. L. Raja, R. J. Kee, O. Deutschmann, J. Warnatz and L. D. Schmidt, "A critical evaluation of Navier-Stokes, boundary-layer, and plug-flow models of the flow and chemistry in a catalytic-combustion monolith," *Catalysis Today*, Vol. 59, No. 1-2 (2000), pp. 47-60.
11. D. Chatterjee, O. Deutschmann and J. Warnatz, "Detailed surface reaction mechanism in a three-way catalyst," *Faraday Discussions*, Vol. 119, (2001), pp. 371-384.
12. F. Laurent, C. J. Pope, H. Mahzoul, L. Delfosse and P. Gilot, "Modelling of NO_x adsorption over NO_x adsorbers," *Chemical Engineering Science*, Vol. 58, No. 9 (2003), pp. 1793-1803.
13. L. Olsson, H. Persson, E. Fridell, M. Skoglundh and B. Andersson, "A Kinetic Study of NO Oxidation and NO_x Storage on Pt/Al₂O₃ and Pt/BaO/Al₂O₃," *Journal of Physical Chemistry B*, Vol. 105, No. 29 (2001), pp. 6895-6906.
14. A. Scotti, I. Nova, E. Tronconi, L. Castoldi, L. Lietti and P. Forzatti, "Kinetic Study of Lean NO_x Storage over the Pt-Ba/Al₂O₃ System," *Industrial & Engineering Chemistry Research*, Vol. 43, No. 16 (2004), pp. 4522-4534.
15. W. S. Epling, G. C. Campbell and J. E. Parks, "The effects of CO₂ and HO on the NO_x destruction performance of a model NO_x storage/reduction catalyst," *Catalysis Letters*, Vol. 90, No. 1-2 (2003), pp. 45-56.
16. Lange, Norbert A. and Dean, John A., *Lange's handbook of chemistry 15th ed.* (New York: McGraw-Hill, 1999).
17. E. Fridell, H. Persson, L. Olsson, B. Westerberg, A. Amberntsson and M. Skoglundh, "Model studies of NO_x storage and sulphur deactivation of NO_x storage catalysts," *Topics in Catalysis*, Vol. 16/17, No. 1-4 (2001), pp. 133-137.
18. C. Sedlmair, K. Seshan, A. Jentys and J. A. Lercher, "Elementary steps of NO_x adsorption and surface reaction on a commercial storage-reduction catalyst," *Journal of Catalysis*, Vol. 214, No. 2 (2003), pp. 308-316.
19. L. Olsson and E. Fridell, "The Influence of Pt Oxide Formation and Pt Dispersion on the Reactions NO₂ ⇌ NO + 1/2 O₂ over Pt/Al₂O₃ and Pt/BaO/Al₂O₃," *Journal of Catalysis*, Vol. 210, No. 2 (2002), pp. 340-353.
20. Hayes, R. E. and Kolaczkowski, S. T., *Introduction to catalytic combustion* (Amsterdam: Gordon & Breach, 1997).
21. O. Deutschmann, S. Tischer, C. Correa, D. Chatterjee, S. Kleditzsch, V. M. Janardhanan, DETCHEM software package, 2.0 ed., www.detchem.com, Karlsruhe, 2004.
22. V. Schmeißer, J. de Riva Pérez, U. Tuttlies and G. Eigenberger, "Experimental results on the role of Pt, Rh, Ba, Ce and Al₂O₃ on NO_x-storage catalyst behaviour." CAPoC7 proceedings - Topics in Catalysis (accepted).

23. L. Lietti, P. Forzatti, I. Nova and E. Tronconi, "NO_x Storage Reduction over Pt-Ba/γ-Al₂O₃ Catalyst," Journal of Catalysis, Vol. 204, No. 1 (2001), pp. 175-191.

CONTACT

Olaf Deutschmann

Institute for Chemical Technology
and Polymer Chemistry
University of Karlsruhe, Germany
Tel: +49 (0) 721 608-3064
Fax: +49 (0) 721 608-4805
Email: deutschmann@ict.uni-karlsruhe.de

NOTATION

A_f pre-exponential factor
 $c_{p,i}$ specific heat at constant pressure of species i
 d channel (tube) diameter
 $D_{i,m}$ diffusion coefficient of species i in the mixture
 D diffusion coefficient within the barium particle
 E_a activation energy
 $F_{cat/geo}$ ratio between catalytic active surface area and geometric surface area
 h_i enthalpy of species i
 k_f, \tilde{k}_f rate constants, forward reaction
 k_b, \tilde{k}_b rate constant, backward reaction
 K^{eq} equilibrium constant
 K_s number of elementary surface reactions (including adsorption and desorption)
 \tilde{M}_i molar mass of the species i
 N_g number of gas phase species
 N_s number of adsorbed species

p static pressure
 $r_{Nitrate}$ position of the nitrate front within the particle
 r_{tot} radius of the barium particle
 R_i net rate of production of species i due to chemical reactions
 R radial spatial coordinate
 R gas constant
 S_0 initial sticking coefficient
 \dot{S}_i creation or depletion rate of species i by adsorption and desorption processes/ chemical source term
 $\dot{s}_i \tilde{M}_i$ surface mass fluxes
 T temperature
 T time
 u axial velocity
 v radial velocity
 X_i concentration of an adsorbed species
 Y_i mass fraction of species i
 z axial spatial coordinate
 \dot{j}_{ir} diffusive flux
 v_{st} Stefan velocity
 $\Delta_R H$ reaction enthalpy
 $\Delta_R S$ reaction entropy
 Γ surface site density
 ε_k parameter for coverage dependent activation energy
 Θ_i surface coverages (fraction of surface sites covered by species i)
 μ viscosity
 μ_{ik} parameter for coverage dependent reaction order
 ν_{ik}, ν'_{jk} stoichiometric coefficients
 ρ density
 τ inhibition term